High resolution carbon cycle and seawater temperature evolution during the Early Jurassic (Sinemurian–Early Pliensbachian)

Gregory D. Price[1], Sarah J. Baker[1, 2], Justin VanDeVelde[1] and Marie-Emilie Clémence[1, 3]

1 School of Geography, Earth & Environmental Sciences, Plymouth University, Drake Circus, Plymouth, PL4 8AA, United Kingdom (g.price@plymouth.ac.uk)

2 University of Exeter, North Park Road, Exeter,EX4 4QE, UK

3 Innsbruck, Institute of Geology, Faculty of Geo- Atmospheric Sciences, Innsbruck, Austria

The Early Jurassic was marked by a progressive recovery from the end-Triassic mass extinction and punctuated by recurring episodes of anoxia. These changes, associated with fluctuations in carbon isotope composition of marine carbonates, remain incompletely understood. Here we present a high-resolution carbon and oxygen isotope record for the Early Jurassic based on well-preserved marine mollusks (belemnites) from Dorset, UK. Our new data show a number of $\delta^{13}C$ excursions, starting with a negative excursion at the Sinemurian–Pliensbachian boundary Event followed by lesser negative excursions showing in the Polymorphous, Jamesoni and Masseanum-Valdani Subzones. The recognition of the Sinemurian–Pliensbachian boundary Event in this study and elsewhere suggests that observed carbon-isotope trends are likely to represent a supra regional perturbation of the carbon cycle. A prominent positive carbon isotope event is also seen within the Pliensbachian Ibex Zone. This event is also clearly evident in the data from belemnites from Spain. This carbon isotope excursion is not, however, coincident with inferred peak temperatures. The oxygen isotope and Mg/Ca data allows the determination of a number of pronounced Pliensbachian cool events. From the low point in the Brevispina Subzone, oxygen isotopes become more negative coupled with an increase in Mg/Ca values culminating in an Early Pliensbachian thermal maximum

during the Davoei Zone. Taken with existing data it appears that the Pliensbachian is characterized by 2 major warmings, firstly within the Davoei Zone followed by warming beginning in the latest Pliensbachian and peaking in the Early Toarcian.

1. Introduction

The Early Jurassic was a dynamic period of Earth history that witnessed significant fluctuations in global ocean chemistry and climate [e.g. van de Schootbrugge et al., 2005a; Bodin et al., 2010; Suan et al., 2010; Korte and Hesselbo, 2011; Dera et al., 2011; Bartolini et al., 2012]. Early Jurassic marine carbon-isotope records show large positive and negative excursions (e.g. the Toarcian Oceanic Anoxic Event), suggesting major perturbations to the carbon cycle caused by increased rates of organic matter deposition as well as the introduction of isotopically light carbon into the ocean–atmosphere system [e.g. Bailey et al., 2003; Hesselbo et al., 2007; Kemp et al., 2005]. The increasing number of high resolution studies has led to similar, but smaller scale events being recognised (e.g. during the Early Sinemurian, Porter et al., 2014]; Late Sinemurian-Early Pliensbachian [van de Schootbrugge et al., 2005a; Woodfine et al., 2008; Korte and Hesselbo 2011; Silva et al., 2011; Riding et al., 2013; Franceschi et al., 2014; Duarte et al., 2014; Silva and Duarte, 2015 Gómez et al., 2016] and at the Pliensbachian–Toarcian boundary [Bodin et al., 2010; Littler et al., 2010]. Hence it appears that Jurassic climates were rather prone to transient change [Riding et al., 2013]. The global significance or regionality of some these events has yet to be fully explored and some intervals of the Jurassic are less well constrained. This study examines the carbon and oxygen isotope record from the Late Sinemurian–Early Pliensbachian from the classic Dorset coast succession of the UK. The abundance of belemnites and common ammonites allows subdivision at the subzonal level and in conjunction with an orbital cycle chronology for the Belemnite Marls [Weedon and Jenkyns, 1990; 1999) allows the scrutiny of perturbations to the carbon cycle, examination of rate of change and the coeval oxygen isotope response.

2. Geologic Setting

Samples for this study were derived from the cliff exposures along the Dorset coast between Charmouth and Seatown in southern UK (Fig. 1). Exposed here are marine sediments of the Charmouth Mudstone Formation of Sinemurian and Pliensbachian age that have been investigated extensively in terms of their biostratigraphy [e.g. Lang and Spath 1926; Lang et al., 1928; Cope et al., 1980; Hesselbo and Jenkyns, 1995; Page, 1992; Simms et al., 2004], lithostratigraphy and sedimentology [e.g. Sellwood, 1972; Cox et al., 1999] carbonate content, total organic-carbon (TOC) and organic carbon-isotope (δ^{13}Corg) composition [Weedon and Jenkyns 1999; Jenkyns and Weedon 2013]. There are a number of major and minor hiatuses within the Charmouth Mudstone Formation, e.g. at the Coinstone level (Bed 89 of Lang et al., 1928], where three ammonite Subzones (Oxynotum, Simpsoni and Denotatus Subzones) are missing [Hesselbo and Jenkyns, 1995], at the Hummocky level (Bed 103), where the 2 highest Subzones of the Raricostatum Zone (the Aplanatum and Macdonnelli) are missing, whilst the Belemnite Stone (Bed 121), is greatly condensed, with the Luridum Subzone just 4-5 cm thick (see Fig. 2). Strontium isotope data [Jones et al., 1994] also indicates a small gap is likely to be present within the Valdani Subzone.

The sediments of the Black Ven Marl Member (of the Charmouth Mudstone Formation) are comprised of medium and dark grey, organic carbon–rich claystones and shales with a few thin limestone and nodule beds. The Birchi Tabular Bed is at the base of the member with the Shales-with-'Beef' Member below. The Black Ven Marl Member typically shows no obvious visible evidence for cyclicity. The overlying Belemnite Marls, separated from the Black Ven Marl Member by the Hummocky level, consists principally of interbedded calcareous claystones and calcareous, organic carbon-rich laminated claystones (Fig. 2). The variations in the content of calcium carbonate, clay, and organic matter lead to the pronounced decimetre-scale light to dark blue-grey bedding Milankovitch forced couplets [Weedon and Jenkyns 1990, 1999]. Weedon and Jenkyns [1999] suggest these couplets result from changes in carbonate productivity and/or clay flux throughout the deposition of the Belemnite Marls. Overlying the Belemnite Marls are the Green Ammonite Beds, which consist of silty grey mudstones that show faint cyclicity in the basal few meters (Fig. 2). Together, these three members represent part of the fill of a half-graben system that constitutes a segment of the Wessex Basin [Chadwick, 1986; Hesselbo and Jenkyns, 1995] and represent transgressive, relatively deep-water facies, or the first marine sediments after a hiatus [Sellwood, 1972]. Deposition occurred in an epeiric seaway that covered much of Europe, and at paleolatitude of ~35°N [Scotese, 2014, Fig. 1). Water depths in southern UK were probably from tens to a few hundred meters [Sellwood and Jenkyns, 1975].

3. Materials and methods

Belemnites samples were collected bed-by-bed and whenever possible, multiple samples were collected from each bed. The belemnite specimens were largely *Nannobelus*, *Hastites*, *Bairstowius* and *Passaloteuthis* (Appendix A) and with the exception of *Nannobelus* often co-occurring at the same stratigraphic level. As documented by Doyle [2002], *Passaloteuthis* has a medium to large cylindrical rostra (typically up to 140 mm), whilst *Hastites* is small sized, slender and has a markedly hastate rostra. *Bairstowius* is medium sized, elongate (typically up to 150mm and a 3-4 mm diameter rostrum), and hastate to subhastate, whereas *Nannobelus* has a small to medium conical to cylindrical rostra. The preservation of the belemnite rostra was assessed using cathodoluminescence (CL) using a MK5 CITL instrument and trace element analysis (Ca, Sr, Mg, Fe and Mn concentrations). The belemnites were prepared for stable isotope and trace element analysis by first removing the areas of the rostrum typically most prone to diagenesis (the rostrum exterior, apical region, alveolus and observable cracks/fractures). The remaining calcite was then fragmented, washed in pure water and dried in a clean environment. Using 300 to 400 micrograms of carbonate, stable isotope data were generated on a VG Optima mass spectrometer with a Gilson autosampler at Plymouth University. Isotope ratios were calibrated using NBS standards and are given in δ notation relative to the Vienna Pee Dee Belemnite (VPDB). Reproducibility was generally better than 0.1‰ for samples and standard materials. The sub-samples taken for trace element (Ca, Mg, Ca, Fe and Mn) analysis were digested in HNO_3 and analyzed by Inductively Coupled Plasma-Atomic Emission Spectrometer (ICP-AES) using a PerkinElmer 3100. Based upon analysis of duplicate samples reproducibility was better than ± 3% of the measured concentration of each element. Repeat analyses of standards JLS-1 and BCS CRM 393 was within 2% of the certified values for Sr, Mn, Ca and Mg and 10% for Fe.

4. Results

The belemnites sampled in this study were mostly translucent, honey colored calcite. CL indicated that most parts of the rostrum were non-luminescent. Some areas were revealed to be Mn-rich and partial replacement by diagenetic calcite was observed particularly along the outermost growth bands and adjacent to the alveolar region (Fig. 3). As noted above areas such as these were either removed prior to or avoided during subsampling. The determined elemental ranges of belemnite rostra (Appendix A) were as follows: Ca (10.2 – 45.8 %); Sr (408–2161 ppm); Mn (1 – 291 ppm); Mg (1267 – 7111 ppm) and Fe (11 – 3263 ppm). Low Mn (<100 ppm) and Fe (<250 ppm) values are recorded for most of the belemnites. Those samples where Fe concentrations were >250 ppm and Mn concentrations >100 ppm [cf. Wierzbowski, 2004; Price and Page, 2008] were considered likely to have undergone some isotopic exchange registered by the precipitation of post-depositional diagenetic calcite and were hence excluded from any further analysis. Fe and Mn concentrations are typically higher in diagenetically altered calcite, as Fe^{2+} and Mn^{2+} are more soluble under reducing conditions and thus available for replacing Ca^{2+} in the calcite lattice [Brand and Veizer 1980]. The highest concentrations are observed in those samples derived from the condensed Belemnite Stone (Bed 121), of the Luridum Subzone.

All $\delta^{13}C$ and $\delta^{18}O$ data are provided as supplementary material (Appendix A). A cross plot of the $\delta^{18}O$ and $\delta^{13}C$ data from the belemnite specimens (*Nannobelus*, *Hastites*, *Bairstowius* and *Passaloteuthis*) is shown in Figure 4. The oxygen isotope data derived from the well-preserved Late Sinemurian and Early Pliensbachian belemnites show an overlapping range of values (-4.5 to 0.9 ‰) and no appreciable difference between genera. Carbon-isotope values recorded from the well-preserved Late Sinemurian to Early Pliensbachian belemnites range from -2.9 up to 4.0‰. Notably the mean (0.6‰) and the range (-1.1 to 4.0‰) for *Passaloteuthis* differs from the mean (-0.8‰) and range (-1.9 to 0.6 ‰) of *Bairstowius.* Using a Student T-test this difference is statistically significant at p. 0.05.

Oxygen ratios through the entire section show both short- and long-term variation and are presented in Figure 5. Within the Sinemurian part of the section examined (the Black Ven Marls) the oxygen isotope data show initially relatively negative values (-2.4 to -0.7‰) and become more positive within the lowermost part of the Pliensbachian and fluctuate in the upper part of the succession (Jamesoni Zones to Ibex Zones) before becoming increasingly negative within the lowermost part of the Green Ammonite Beds. Here a ~2 ‰ shift towards negative values is seen within the Davoei Zone. Although the carbon-isotope data show a degree of scatter, again a series of events are observed up through the section. Consistently positive carbon isotope values are recorded for the Sinemurian. A change to negative carbon isotope values is seen across the Sinemurian–Pliensbachian boundary, followed by a series of smaller negative–positive oscillations, culminating with a large ~ 4.0‰ positive shift with the Valdani Subzone. Also shown in Figure 5 are the Mg/Ca (mmol/mol) ratios of the belemnites. Mg/Ca ratios increase upwards across the Sinemurian–Pliensbachian boundary with notable peaks in the Polymorphous Subzone. Following a low point in the Brevispina Subzone, Mg/Ca ratios again increase upwards.

5. Discussion

5.1 The Sinemurian–Pliensbachian Event

On the basis of the proposed stratigraphic framework, the Dorset $\delta^{13}C_{belemnite}$ curve displays a series of distinctive features that show both long-term and short term trends in isotopic and elemental data as outlined above. These can be correlated with existing coeval $\delta^{13}C$ records from different geologic settings (Fig. 6). The first such carbon isotope event is seen crossing the Sinemurian–Pliensbachian boundary. Despite the two highest Raricostatum Subzones of the Zone missing in Dorset, a pronounced shift to more negative carbon values is clearly apparent. Comparable studies [e.g. Hesselbo et al., 2000; Woodfine et al., 2008; Korte and Hesselbo, 2011; Duarte et al., 2014; Franceschi et al., 2014] also recognise a Sinemurian–Pliensbachian boundary event from UK belemnite-based datasets as well as carbonate carbon data from Atlantic and Tethyan basins and the organic $\delta^{13}C$ record of van de Schootbrugge et al. [2005a] from the Mochras Borehole, UK. A pronounced shift to more negative carbon values is also recorded in belemnite calcite from the Asturian Basin of Northern Spain [Gómez et al., 2016]. Perhaps of significance is that the most negative values seen here represent some of the most negative values for the entire Jurassic [see for example Jenkyns et al., 2002; Suan et al., 2010; Korte and Hesselbo, 2011; Dera et al., 2011]. From the Portuguese reference section of

San Pedro de Moel (Lusitanian Basin) carbon isotope data of Duarte et al. [2014] from bulk carbonates, also shows a negative excursion beginning in the Raricostatum Zone. Equally, carbon isotope data from the Southern Alps of northern Italy, the Madonna della Corona section [Woodfine et al., 2008] and the Viote section [Franceschi et al., 2014] show a negative carbonate isotope excursion at the Sinemurian–Pliensbachian boundary. Despite the differences in facies between the sections, due to deposition under different environmental conditions across the region, the $\delta^{13}C$ signatures are similar. The carbon-isotope trends are therefore likely to represent a supra regional perturbation of the carbon cycle. Moreover these observations preclude the possibility that the Sinemurian–Pliensbachian event was restricted to an isolated seaway or basin resulting from transient carbon perturbations producing non uniform and spatially heterogeneous carbon isotope changes in the ocean [c.f. Harazim et al., 2013]. Hence, wider scale mechanisms need to be considered to account for the observed trends. If we accept a quasi-global nature of this carbon isotope event, then a source for light carbon must have existed to produce such a negative excursion.

Similar negative carbon isotope excursions in the geologic record have been explained by the injection of isotopically light carbon into the ocean and atmosphere from remote sources, such as methane from clathrates, wetlands, or thermal metamorphism organic rich sediments [e.g., Svensen et al., 2004; McElwain et al., 2005; Hesselbo et al., 2007; Bodin et al., 2010; Bachan et al., 2012]. Alternatively, the Toarcian negative carbon isotope excursion has been considered to be a more regional event caused by recycling of isotopically light carbon from the lower water column [e.g. Schouten et al., 2000; van de Schootbrugge et al., 2005b; McArthur et al., 2008]. Coincident with the Early Toarcian event, a distinct minimum in $\delta^{18}O$ values derived from belemnites and a maximum in Mg/Ca ratios, is interpreted as a significant paleotemperature increase [Bailey et al., 2003]. A similar trend is also recorded by Suan et al. [2010] in brachiopod calcite from the Lusitanian Basin of Portugal.

The oxygen isotopes of this study can clearly contribute to understanding the mechanisms behind the Sinemurian–Pliensbachian carbon cycle perturbation. Assuming equilibrium precipitation of calcite, oxygen isotope compositions of shells are largely controlled by a combination of temperature and the $\delta^{18}O$ of seawater. Where continental ice volume is at a minimum and evaporation or freshwater inputs are minor factors, increasingly negative $\delta^{18}O_{belemnite}$ values can be correlated with elevated temperatures and vice versa. The oxygen isotope data of this study (incorporating the data of Jenkyns et al., 2002 from Dorset) across the Sinemurian–Pliensbachian boundary (Fig. 5) show a marked positive excursion that could therefore indicate a cooling of seawater. A cooling trend through the latest Sinemurian is consistent also with the data of Hesselbo et al. [2000] and Korte and Hesselbo [2011] from the Cleveland Basin of the UK. Korte and Hesselbo [2011] suggest that one possible explanation is that seafloor temperatures became cooler across the Sinemurian–Pliensbachian boundary in the Cleveland Basin because of deepening of the depositional environment that has been inferred from facies and biofacies evidence. Alternatively a change towards more positive seawater $\delta^{18}O$ values would require an increase in evaporation across the Sinemurian–Pliensbachian boundary. A cooling trend through the latest Sinemurian is also seen within the data of Silva et al. [2011] from Portugal and Gómez et al. [2016] from Spain. A cooling trend through the latest Sinemurian is also consistent with a climate (glacio-eustatic) forcing of the sea level. Evidence for a Late Sinemurian sea-level fall followed by a Pliensbachian transgression is a widespread feature [e.g. Hallam, 1988]. Similar sea-level variations are seen in the UK [Hesselbo and Jenkyns, 1995], the Lusitanian Basin [Plancq et al., 2016] and Greenland [Surlyk, 1991].

Hence it seems possible that the negative carbonate isotope excursion at the Sinemurian–Pliensbachian boundary is a supra-regional event associated with an influx ^{12}C-rich and cold waters. As noted above, the recycling/upwelling of isotopically light carbon from the lower parts of the water column [van de Schootbrugge et al., 2005b] has been considered to account for the Toarcian isotopic event [cf. Hesselbo et al., 2007]. The key difference here is that the belemnites of this study are recording both light carbon and positive oxygen isotopes (cooler temperatures), whereas associated with Early Toarcian event, as noted above, belemnites indicate warm seawater temperatures [e.g., McArthur et al., 2000; Bailey et al., 2003; Jenkyns, 2010].

Another potential temperature proxy in our dataset is the Mg content of the belemnites. The magnesium concentration in calcite depends on ambient seawater temperature and increases with warming [e.g., Katz, 1973], a relationship that has been widely exploited in foraminifers as a paleothermometer [e.g., Lear et al., 2002] as well as belemnites [e.g., Bailey et al., 2003; Rosales et al., 2004; Nunn and Price, 2010; Price, 2010; Armendáriz et al., 2012; 2013]. Unlike $\delta^{18}O$, Mg/Ca ratios are thought to be largely unaffected by salinity [e.g., Yasamanov, 1981]. Rather puzzlingly, the Mg/Ca data [Fig. 5] across the Sinemurian–Pliensbachian boundary show no marked inflection, indicative of cooling (or warming). Some studies have shown of a lack of correlation between Mg/Ca and $\delta^{18}O$ in some belemnite species [McArthur et al., 2007; Li et al., 2012; Sørensen et al., 2015] and have therefore questioned the validity of Mg/Ca ratios as useful paleotemperature indicator.

5.2 Pliensbachian Carbon Isotope events

Following the Sinemurian–Pliensbachian Event, a trend towards more positive $\delta^{13}C_{carb}$ values is seen. This return to more positive δ^{13}Ccarb values, is again followed by a number of more minor negative excursions showing in the smoothed data in the Polymorphous, Jamesoni and Masseanum-Valdani Subzones. Of note is that these carbon isotope trends are either derived from mixed belemnites species or not related simply to a switch from one species to another (c.f. Fig. 4). Similar scale events are possibly recognisable, although less well constrained in terms of biostratigraphy in other sections [e.g. Woodfine et al., 2008; Franceschi et al., 2014]. Because a cyclostratigraphic timescale for the Belemnite Marls has been developed [Weedon and Jenkyns, 1999] this allows constraints to be placed on the minimum duration of Early Pliensbachian ammonite Zones and Subzones and therefore also of the negative excursions. Thus for the Sinemurian–Pliensbachian Event, although possibly incomplete as a result of erosion and/or non-deposition (see above), the durations is ∼ 105 kyr. For the excursion within the Jamesoni Subzone, the duration is ∼190 kyr and the excursion within Masseanum-Valdani Subzones is ∼130 kyr. These inferred durations are a little shorter that other negative isotope events. For example, the Toarcian negative carbon-isotope excursion has been estimated to have a duration between 200 and 1000 kyr [e.g. McArthur et al., 2000; Kemp et al., 2005; Huang and Hesselbo, 2014], whilst a prominent Oxfordian negative carbon isotope excursion has been estimated to have a duration of ∼200 kyr [Padden et al., 2001].

A prominent positive carbon isotope event is also seen within the Ibex Zone (uppermost Valdani Subzone). This event is clearly evident in the data for this interval reported by Rosales et al. [2006] from belemnites from the Basque–Cantabrian (Fig. 6). and from the Asturian basins, Spain [Armendáriz et al., 2012; Gómez et al., 2016]. Small positive excursions are possibly seen also in the data from Woodfine et al. [2008] and Franceschi et al. [2014] although subzonal biostratigraphic control is lacking for these sections. Within the $\delta^{13}C$ records derived from bulk carbonate from Peniche, Portugal [Oliveira et al., 2006] this positive carbon isotope event is also possibly present (Fig. 6). As belemnite $\delta^{13}C$ records usually track $\delta^{13}C$ curves derived from bulk carbonates [e.g. Price and Mutterlose, 2004; Hesselbo et al., 2007; Wierzbowski et al., 2009] confirming the persistence of these trends across different carbonate substrates.

Other significant positive carbon isotope excursions of the Jurassic and Cretaceous have been linked to enhanced organic matter burial as a cause [e.g., Schouten et al., 2000; Jenkyns et al., 2002; Locklair et al., 2011]. Whether this positive carbon isotope excursion is due to enhanced organic carbon burial is somewhat speculative given the absence of a noticeable peak in organic carbon/black-shale deposition. Although, Weedon and Jenkyns [1999] and Jenkyns and Weedon [2013] report relatively high TOC values for the Black Ven Marls (up to 12 wt. %) and the Belemnite Marls (up to 6 wt. %) the prominent positive carbon isotope event of the uppermost Valdani Subzone does not coincide with particularly high TOC values (Fig. 5). Likewise, Rosales et al. [2006] in their study of hemipelagic deposits from northern Spain, note that that positive carbon isotope peaks are preceded (rather than coincident) by increases in the TOC content. In the Lusitanian Basin (Peniche), this level marks the onset of a longer period of black shale deposition (Silva et al., 2011).

Prior to the event seen in the within the Valdani Subzone, the high number of analyses permits a number of other positive events of a lesser magnitude to be identified (e.g., within the Brevispina and Jamesoni Subzones). Hence it appears that the Early Jurassic ocean was rather prone to transient carbon cycling fluctuations [e.g., Riding et al., 2013] although again significant organic carbon burial may not be associated with these events. Mass balance models [e.g. Locklair et al., 2011] suggest only relatively small changes in organic carbon and carbonate accumulation rates are required to produce carbon isotopic excursions of +0.5‰. Using the a cyclostratigraphic timescale of Weedon and Jenkyns [1999] suggests a duration of ~90 to 140 ky per for each excursion.

5.2 Pliensbachian temperature variation

Analysis of the Pliensbachian oxygen isotope data allows the determination of a number of cool events (most positive oxygen values), namely within the Taylori, Polymorphous and

Brevispina subzones. The positive oxygen isotope values (accompanied by low Mg/Ca ratios) of the Brevispina Subzone are not seen in other large datasets [e.g. Jenkyns et al., 2002; Rosales et al., 2004; Dera et al., 2011; Armendáriz et al., 2012], perhaps due to lower sample numbers examined.

The carbon isotope excursion of the Valdani Subzone, noted above, appears coincident with rising with temperatures, although inferred peak temperatures occur within the Maculatum Subzone. From the low point in the Brevispina Subzone, oxygen isotopes become more negative coupled with an increase in Mg/Ca values. Assuming little change in $\delta^{18}O_{seawater}$ and using the Anderson and Arthur [1983] temperature equation, this change in oxygen isotopes represents a warming of ~10°C. An Early Pliensbachian warming event, with a thermal maximum during the Davoei Zone has also been recorded elsewhere [e.g. Dera et al., 2011] although less obvious in the data of Korte and Hesselbo [2011]. These temperature interpretations correlate with inferred sea-level fluctuations whereby an Early Pliensbachian major transgression [e.g. Sellwood, 1972; Haq et al., 1988; Hallam, 1988] with a high in the Ibex-Davoei Zones was followed by a short-lived but prominent regressive episode at the end of the Pliensbachian. Hesselbo and Jenkyns (1995) also suggest that the condensation of the Luridum Subzone to be related to sediment starvation and deepening. As noted above, the highest concentrations of Mn are from samples from the Luridum Subzone and enrichments of Mn in condensed pelagic successions have also been associated with transgressions [e.g. Corbin et al., 2000]. These have been linked to Mn fluxes; lower sedimentation rates and the proximity of the oxic-suboxic boundary in the sediment controlling amount of Mn carbonate formed. Our evidence suggests that peak temperatures, positive carbon isotope events and TOC rich intervals are not, however, synchronous [c.f. Silva and Duarte, 2015]. Two lesser peaks where negative oxygen isotopes are coupled with increases in Mg/Ca ratios are also notable in the Polymorphous Subzone.

6. Conclusions

Our high-resolution data suggests that the Early Jurassic was a dynamic period of Earth history that witnessed significant relatively short term changes in global ocean chemistry. Whereas long term oscillations between cold and warm climates in the Jurassic have been linked with the variation in CO_2 [e.g. Dera et al., 2011; Jenkyns, 2010; Korte and Hesselbo 2011], the character and origins of these shorter term climate variations are not so well understood. A negative $\delta^{13}C$ excursion is recognized at the Sinemurian–Pliensbachian boundary followed by lesser excursions within the Polymorphous, Jamesoni and Masseanum-Valdani Subzones. The recognition of the Sinemurian–Pliensbachian boundary Event in this study and elsewhere suggests trends are likely to represent a supra regional perturbation of the carbon cycle. From a broader perspective, a protracted interval showing changes in carbon cycling is not unique [e.g. Bartolini et al., 2012], as similarities exist between these Early Jurassic events, and other studied Mesozoic intervals that are also interpreted as global. Hence, we speculate that perturbations of the global carbon cycle were not confined to specific intervals (e.g. within the immediate vicinity of an extinction interval), but are rather persistent for substantial lengths of geologic time afterwards. Factors which may have pre-conditioned the Jurassic ocean to be particularly prone to being unstable may have included the paleogeography with abundant shallow seaways, and ongoing volcanism associated with the rifting of the Atlantic.

The oxygen isotope data allows the determination of a number of pronounced Pliensbachian cool events, and an Early Pliensbachian thermal maximum during the Davoei Zone. Taken with existing data it appears that the Pliensbachian is characterized by 2 major warmings, the first of Davoei Zone followed by warming beginning in the latest Pliensbachian and peaking in the Early Toarcian [e.g. Dera et al., 2011].

Acknowledgements

Part of this research was undertaken by SB while an MGeol student funded by Plymouth University. Funding for JV was provided by a Natural Environment Research Council (NERC) grant awarded to GDP (NE/J020842/1). The data used are listed in the references and supporting information. This paper greatly benefited from 2 constructive reviews.

References

Anderson, T.F. and M.A. Arthur, (1983), Stable isotopes of oxygen and carbon and their applications to sedimentological and paleoenviromental problems. In: *Stable Isotopes in Sedimentary Geology* (Arthur, M.A., Anderson, T.F. Kaplan, I.R. Veizer J. and Land, L.S. eds). SEPM, Short Course Notes, 10, 1.1–1.151.

Armendáriz, M., I. Rosales, B. Bádenas, M. Aurell, J.C. García-Ramos, and L. Piñuela (2012), High-resolution chemostratigraphic records from Lower Pliensbachian belemnites: Palaeoclimatic perturbations, organic facies and water mass exchange (Asturian basin, northern Spain). *Palaeogeography, Palaeoclimatology, Palaeoecology*, *333-334,* 178–191.

Armendáriz, M., I. Rosales, B. Bádenas, L. Piñuela, M. Aurell, and J.C. García-Ramos, (2013), An approach to estimate Lower Jurassic seawater oxygen isotope composition using $\delta^{18}O$ and Mg/Ca ratios of belemnite calcites (Early Pliensbachian, northern Spain). *Terra Nova*, 25**,** 439–445.

Bachan, A., B. van de Schootbrugge, J. Fiebig, C.A. McRoberts, C. Ciarapica, J.L. Payne, (2012), Carbon cycle dynamics following the end-Triassic mass extinction: Constraints from paired δ^{13}Ccarb and δ^{13}Corg records. Geochemistry, Geophysics, Geosystems 13, Q09008. doi.org/10.1029/2012GC004150

Bailey, T.R., Y. Rosenthal, J.M. McArthur, B. van de Schootbrugge, and M.F. Thirlwall, (2003), Paleoceanographic changes of the Late Pliensbachian–Early Toarcian interval: A possible link to the genesis of an oceanic anoxic event. *Earth and Planetary Science Letters*, *212*, 307–320.

Bartolini, A., J. Guex, J.E. Spangenberg, B. Schoene, D.G. Taylor, U. Schaltegger, and V. Atudorei, (2012), Disentangling the Hettangian carbon isotope record: Implications for the aftermath of the end-Triassic mass extinction. *Geochemistry Geophysics Geosystems*, 13, Q01007 DOI: 10.1029/2011GC003807

Bodin, S., E. Mattioli, S. Fröhlich, J.D. Marshall, L. Boutib, S. Lahsini, and J. Redfern, (2010), Toarcian carbon isotope shifts and nutrient changes from the Northern margin of Gondwana (High Atlas, Morocco, Jurassic): Palaeoenvironmental implications. *Palaeogeography, Palaeoclimatology, Palaeoecology*, *297*, 377–390.

Brand, U., and J. Veizer, (1980), Chemical diagenesis of a multicomponent carbonate system.1. Trace-elements. *Journal of Sedimentary Petrology*, *50*, 1219–1236

Chadwick, R., (1986), Extension tectonics in the Wessex Basin, southern England. *Journal of the Geological Society, London*, *143*, 465–488.

Cope, J.C.W., T.A. Getty,. M.K. Howarth, N. Morton and H.S. Torrens, (1980), A Correlation of Jurassic Rocks in the British Isles. Part One: Introduction and Lower Jurassic. *Special Report of the Geological Society of London 14*, 1–73.

Corbin, J.C., A. Person, A. Iatzoura, B. Ferre, and M. Renard, (2000), Manganese in pelagic carbonates: Indication of major tectonic events during the geodynamic evolution of a passive continental margin (the Jurassic European Margin of the Tethys-Ligurian Sea). *Palaeogeography, Palaeoclimatology, Palaeoecology*, *156*, 123–138.

Cox, B.M., M.G. Sumbler, and H.C. Ivimey-Cook, (1999), A formational framework for the Lower Jurassic of England and Wales (onshore area). Brit. Geol. Surv. Res. Rept., RR/99/01.

Dera, G., B. Brigaud, F.Monna, R. Laffont, E. Pucéat, J.-F. Deconinck, P. Pellenard, M.M. Joachimski, and C. Durlet, (2011), Climatic ups and downs in disturbed Jurassic world, *Geology 39*, 215–218.

Doyle, P., (2002), Mollusca – Belemnites. In Lord, A.R. and Davis, P. G. Fossils from the Lower Lias of the Dorset Coast The Palaeontological Association Field Guide to Fossils, *13*, 262–275.

Duarte, L.V., M.J. Comas-Rengifo, R.L. Silva, R. Paredes, and A. Goy, (2014), Carbon isotope stratigraphy and ammonite biochronostratigraphy across the Sinemurian–Pliensbachian boundary in the western Iberian margin. *Bulletin of Geosciences 89*, 719–736.

Franceschi, M., J. Dal Corso, R. Posenato, G. Roghi, D. Masetti, and H.C. Jenkyns, (2014), Early Pliensbachian (Early Jurassic) C-isotope perturbation and the diffusion of the Lithiotis Fauna: Insights from the western Tethys. *Palaeogeography, Palaeoclimatology, Palaeoecology*, *410*, 255–263.

Gómez, J.J., M.J. Comas-Rengifo, and A. Goy, (2016), Palaeoclimatic oscillations in the Pliensbachian (Lower Jurassic) of the Asturian Basin (Northern Spain). *Clim. Past, 12,* 1199–1214.

Hallam, A., (1988), A re-evaluation of Jurassic eustasy in the light of new data and the revised Exxon curve. In: Wilgus, C.K., B.S. Hastings, C.A. Ross, H. Posamentier, J. Van Wagoner and C.G.St.C. Kendall, (Eds.), Sea-level changes: an integrated approach. *Society of Economic Paleontologists and Mineralogists, Special Publications*, *42*, 261–273.

Haq, B.U., J. Hardenbol, and P.R. Vail, (1988), Mesozoic and Cenozoic chronostratigraphy and cycles of sea-level change. In: Wilgus, C.K., B.S. Hastings, C.A. Ross, H. Posamentier, J. Van Wagoner and C.G.St.C. Kendall, (Eds.), Sea-level changes: an integrated approach. *Society of Economic Paleontologists and Mineralogists, Special Publications*, *42*, 71-108.

Harazim, D., B. van de Schootbrugge, K. Sorichter, J. Fiebig, A. Weug, G. Suan and W. Oschmann, (2013), Spatial variability of watermass conditions within the European Epicontinental Seaway during the Early Jurassic (Pliensbachian–Toarcian). *Sedimentology*, *60,* 359–390.

Hesselbo, S.P., C. Meister, & D.R. Gröcke, (2000), A potential globalstratotype for the Sinemurian–Pliensbachian boundary (Lower Jurassic), Robin Hood's Bay, UK: Ammonite faunas and isotope stratigraphy. *Geological Magazine, 137*, 601–607.

Hesselbo, S.P., H.C. Jenkyns, L.V. Duarte, and L.C.V. Oliveira, (2007), Carbon-isotope record of the Early Jurassic (Toarcian) Oceanic Anoxic Event from fossil wood and marine carbonate (Lusitanian Basin, Portugal). *Earth and Planetary Science Letters, 253*, 455–470.

Hesselbo, S.P. and H.C. Jenkyns, (1995), A comparison of the Hettangian to Bajocian successions of Dorset and Yorkshire, in Taylor P. D., ed., Field geology of the British Jurassic: *Geological Society of London,* p. 105–150.

Huang, C. and S.P. Hesselbo, (2014), Pacing of the Toarcian Oceanic Anoxic Event (Early Jurassic) from astronomical correlation of marine sections. *Gondwana Research 25*, 1348–1356.

Jenkyns, H.C. (2010). Geochemistry of oceanic anoxic events. *Geochemistry Geophysics Geosystems*, 11, Q03004

Jenkyns, H.C. and G.P. Weedon, (2013), Chemostratigraphy ($CaCO_3$, TOC, δ^{13}Corg) of Sinemurian (Lower Jurassic) black shales from the Wessex Basin, Dorset and palaeoenvironmental implications. *Newsletters on Stratigraphy*, *46,* 1–21.

Jenkyns, H.C., C.E. Jones, D.R. Gröcke, S.P. Hesselbo, and D.N. Parkinson, (2002), Chemostratigraphy of the Jurassic system: applications, limitations and implications for palaeoceanography. *Journal of the Geological Society, London, 159*, 351–378.

Jones, C.E., H.C. Jenkyns, & S.P. Hesselbo, (1994), Strontium isotopes in Early Jurassic seawater: *Geochimica et Cosmochimica Acta*, *58*, 1285–1301.

Katz, A., (1973), The interaction of magnesium with calcite during crystal growth at 25–90°C and one atmosphere. *Geochimica et Cosmochimica Acta*, *37*, 1563–1586.

Kemp, D.B., A.L. Coe, A.S. Cohen, and L. Schwark, (2005), Astronomical pacing of methane release in the Early Jurassic period. Nature, *437*, 396–399.

Korte, C. and S.P. Hesselbo, (2011), Shallow marine carbon and oxygen isotope and elemental records indicate icehouse-greenhouse cycles during the Early Jurassic. *Paleoceanography*, *26*, PA4219, doi:10.1029/2011PA002160

Lang, W.D. and L.F. Spath, (1926), The Black Marl of Black Ven and Stonebarrow, in the Lias of the Dorset Coast. *Quarterly Journal of the Geological Society, London*, *82*, 144–187.

Lang, W.D., L.F. Spath, L.R. Cox, and H.M. Muir-Wood, (1928), The Belemnite Marls of Charmouth, a series in the Lias of the Dorset coast. *Quarterly Journal of the Geological Society, London 84*, 179-257.

Lear, C.H., Y. Rosenthal, and N. Slowey, (2002), Benthic foraminiferal Mg/Ca paleothermometry: a revised core-top calibration. Geochimica et Cosmochimica Acta, *66*, 3375–3387.

Li, Q., J.M. McArthur, P. Doyle. N. Janssen, M.J. Leng, W. Müller and S. Reboulet, (2013), Evaluating Mg/Ca in belemnite calcite as a palaeo-proxy. *Palaeogeography Palaeoclimatology Palaeoecology*, *388*, 98–108.

Littler, K., S.P. Hesselbo, and H. C. Jenkyns, (2010), A carbon-isotope perturbation at the Pliensbachian–Toarcian boundary: Evidence from the Lias Group, NE England. *Geological Magazine*, *147*, 181–192.

McArthur, J.M., D.T. Donovan, M.F. Thirlwall, B.W. Fouke, and D. Mattey, (2000), Strontium isotope profile of the early Toarcian (Jurassic) Oceanic Anoxic Event, the duration of ammonite biozones, and belemnite palaeotemperatures. *Earth and Planetary Science Letters 179*, 269–285.

McArthur, J.M., P. Doyle, M.J. Leng, K. Reeves, C.T. Williams, R. García-Sánchez, and R.J. Howarth, (2007), Testing palaeo-environmental proxies in Jurassic belemnites: Mg/Ca, Sr/Ca, Na/Ca, $\delta^{18}O$ and $\delta^{13}C$. *Palaeogeography, Palaeoclimatology, Palaeoecology*, *252*, 464–480.

McArthur, J.M., T.J. Algeo, B. van de Schootbrugge, Q. Li, and R.J. Howarth, (2008). Basinal restriction, black shales, and the Early Toarcian (Jurassic) oceanic anoxic event. *Paleoceanography 23*, PA4217.

McElwain, J.C., J. Wade-Murphy, and S.P. Hesselbo, (2005), Changes in carbon dioxide during an oceanic anoxic event linked to intrusion into Gondwana coals. *Nature*, *435*, 479–482.

Nunn, E.V. and G.D. Price (2010), Late Jurassic (Kimmeridgian–Tithonian) stable isotopes ($\delta^{18}O$, $\delta^{13}C$) and Mg/Ca ratios: new palaeoclimate data from Helmsdale, northeast Scotland. *Palaeogeography, Palaeoclimatology, Palaeoecology*, *292*, 325–335.

Oliveira, L.C.V., R. Rodrigues, L.V. Duarte, and V., Lemos (2006), Avaliação do potencial gerador de petróleo e interpretação paleoambiental com base em biomarcadores e isótopos estáveis do carbono da seção Pliensbaquiano-Toarciano inferior (Jurássico inferior) da região de Peniche (Bacia Lusitânica, Portugal). *Bol. Geociências Petrobras 14,* 207-234

Padden, H., H. Weissert, and M. DeRafelis, (2001), Evidence for Late Jurassic release of methane from gas hydrate. *Geology*, *29*, 223–226.

Page, K.N., (1992), The sequence of ammonite correlated horizons in the British Sinemurian. *Newsletters on Stratigraphy, 27*, 129–156.

Plancq, J., E. Mattioli, B. Pittet, F. Baudin, L.V. Duarte, M. Boussaha, V. Grossi, (2016), A calcareous nannofossil and organic geochemical study of marine palaeoenvironmental changes across the Sinemurian/Pliensbachian (early Jurassic, ~191 Ma) in Portugal. *Palaeogeography, Palaeoclimatology, Palaeoecology*, *449*, 1–12.

Porter, S.J., P.L. Smith, A.H. Caruthers, P. Hou, D.R. Gröcke, and D. Selby, (2014), New high resolution geochemistry of Lower Jurassic marine sections in western North America: A global positive carbon isotope excursion in the Sinemurian? *Earth and Planetary Science Letters*, *397*, 19–31.

Price, G.D., (2010), Carbon-isotope stratigraphy and temperature change during the Early-Middle Jurassic (Toarcian-Aalenian), Raasay, Scotland, UK. *Palaeogeography Palaeoclimatology Palaeoecology*, *285*, 255–263.

Price, G.D. and K.N. Page, (2008), An isotopic analysis of molluscan faunas from the Callovian–Oxfordian boundary at Redcliff Point, Weymouth, Dorset: implications for belemnite behaviour. *Proceedings of the Geologists' Association 119*, 153–160.

Price, G.D. and J. Mutterlose (2004), Isotopic signals from late Jurassic–early Cretaceous (Volgian–Valanginian) subArctic Belemnites, Yatria River, Western Siberia. *Journal of the Geological Society, London*, *161*, 959–968.

Riding, J.B., M.J. Leng, S. Kender, S.P. Hesselbo, and S. Feist-Burkhardt, (2013), Isotopic and palynological evidence for a new Early Jurassic environmental perturbation. *Palaeogeography, Palaeoclimatology, Palaeoecology*, *374*, 16–27.

Rosales, I., S. Quesada, and S. Robles, (2004), Paleotemperature variations of Early Jurassic seawater recorded in geochemical trends of belemnites from the Basque–Cantabrian Basin, northern Spain. *Palaeogeography, Palaeoclimatology, Palaeoecology, 203*, 253–275.

Rosales, I., S. Quesada, and S. Robles, (2006), Geochemical arguments for identifying second-order sea-level changes in hemipelagic carbonate ramp deposits. *Terra Nova*, *18*, 233–240.

Scotese, C.R., (2014), Atlas of Jurassic Paleogeographic Maps, PALEOMAP Atlas for ArcGIS, volume 4, The Jurassic and Triassic, Maps 32-42, Mollweide Projection, PALEOMAP Project, Evanston, IL.

Schouten, S., M.E. Kaam-Peters, I. Rijpstra, M. Schoell, and J.S. Sinnighe Damste, (2000), Effects of an oceanic anoxic event on the stable carbon isotopic composition of early Toarcian carbon. *American Journal of Science*, *300*, 1–22

Sellwood, B.W., (1972), Regional environmental change across a Lower Jurassic stage boundary. *Palaeontology, 15*, 125–157.

Sellwood, B.W. and H.C. Jenkyns, (1975), Basins and swells and the evolution of an epeiric sea (Pliensbachian-Bajocian of Great Britain). *Journal of the Geological Society, London*, *131*, 373–388.

Silva, R.L. and L.V. Duarte (2015), Organic matter production and preservation in the Lusitanian Basin (Portugal) and Pliensbachian climatic hot snaps. *Global and Planetary Change 131*, 24–34.

Silva, R.L., L.V. Duarte, M.J. Comas-Rengifo, J.G. Mendonça Filhoand, A.C. Azerêdo, (2011), Update of the carbon and oxygen isotopic records of the Early–Late Pliensbachian (Early Jurassic, ~187 Ma): insights from the organic-rich hemipelagic series of the Lusitanian Basin (Portugal). *Chem. Geol. 283*, 177–184.

Simms, M.J., J. Chidlaw, N. Morton, and K.N. Page (2004), British Lower Jurassic Stratigraphy. *Geological Conservation Review*, *30*, 458 pp.

Sørensen, A.M., C.V. Ullmann, N. Thibault, C. Korte, (2015), Geochemical signatures of the early Campanian belemnite *Belemnellocamax mammillatus* from the Kristianstad Basin in Scania, Sweden. *Palaeogeography, Palaeoclimatology, Palaeoecology 433*, 191–200.

Suan, G., E. Mattioli, B. Pittet, C. Lécuyer, B. Suchéras-Marx, L.V. Duarte, M. Philippe, F. Reggiani, and F. Martineau, (2010), Secular environmental precursor to Early Toarcian (Jurassic) extreme climate changes. *Earth and Planetary Science Letters 290*, 448–458.

Surlyk, F., (1991), Sequence stratigraphy of the Jurassic–lowermost Cretaceous in East Greenland. *Bulletin of American Association of Petroleum Geologists 75*, 1468–1488.

Svensen, H., S. Planke, A. Malthe-Sorenssen, B. Jamtveit, R. Myklebust, T.R. Eidem, and S.S. Rey, (2004), Release of methane from a volcanic basin as a mechanism for initial Eocene global warming. *Nature 429*, 542–545.

Thierry, J., E. Barrier, M.F. Bergerat, J. Brunet, S. Canerot, S. Crasquin, S. Eli, G. Georgiev, F. Kockel, J. Le Metour, Y.M., Le Nindre, A.M. Nikishin, D.L. Panov, A. Poisson, M. Sandulescu, I., Sapunov, A., Seghedi, M. Soussi, R. Stephenson , P. Tchoumatchenco, D. Vaslet, A. Voznesensky, B. Vrielynck, (2000), Map 8. Middle Toarcian (180–178 Ma). In: Atlas Peri-Tethys Paleogeographical Maps vol. I-XX. (J. Dercourt, M. Gaetani, B., Vrielynck, E. Barrier, B. Biju-Duval, M.-F. Brunet, J.P. Cadet, S. Crasquin and M. Sandulescu, eds). CCGM/CGMW, Paris.

van de Schootbrugge, B., T.R. Bailey, Y. Rosenthal, M.E. Katz, J.D. Wright, K.G. Miller, S Feist-Burkhardt. and P. Falkowski, (2005a), Early Jurassic climate change and the radiation of organic-walled phytoplankton in the Tethys Ocean. *Paleobiology 31*, 73–97.

van de Schootbrugge, B., J.M. McArthur, T.R. Bailey, Y. Rosenthal, J.D. Wright and K.G. Miller, (2005b), Toarcian oceanic anoxic event: an assessment of global causes using belemnite C isotope records. *Paleoceanography*, *20*, PA3008, doi:10.1029/2004PA001102.

Weedon, G.P. and H.C. Jenkyns, (1990), Regular and irregular climatic cycles and the Belemnite Marls (Pliensbachian, Lower Jurassic, Wessex Basin). *Geological Society of London Journal*, *147*, 915–918.

Weedon, G.P. and H.C. Jenkyns, (1999), Cyclostratigraphy and the Early Jurassic timescale: data from the Belemnite Marls, Dorset, south England. *Geological Society of America Bulletin*, *111*, 1823–1843.

Wierzbowski, H., (2004), Carbon and oxygen isotope composition of Oxfordian–Early Kimmeridgian belemnite rostra: palaeoenvironmental implications for Late Jurassic seas. *Palaeogeography, Palaeoclimatology, Palaeoecology 203*, 153–168.

Wierzbowski, H., K. Dembicz, and T. Praszkier, (2009), Oxygen and carbon isotope composition of Callovian-Lower Oxfordian (Middle-Upper Jurassic) belemnite rostra from central Poland: a record of a Late Callovian global sea-level rise? *Palaeogeography Palaeoclimatology Palaeoecology*, *283*, 182–194.

Woodfine, R. G., H.C. Jenkyns, M. Sarti, F. Baroncini, and C. Violante, (2008), The response of two Tethyan carbonate platforms to the Early Toarcian (Jurassic) oceanic anoxic event: Environmental change and differential subsidence. *Sedimentology*, *55*, 1011–1028.

Yasamanov, N.A., (1981), Paleothermometry of Jurassic, Cretaceous, and Paleogene periods of some regions of the USSR. *International Geology Review 23*, 700–706.

Figure 1 Outcrop map for the Lias Group in England and Wales and showing the location of Dorset, UK [after Cox et al., 1999]. Early Jurassic paleogeographic map modified from Thierry et al., [2000].

Figure 2 A. The Belemnite Marls at Westhay Water, Charmouth, UK showing pronounced decimetre-scale light to dark blue-grey Milankovitch forced couplets reflecting variations in the calcium carbonate content B. Sediments of the Black Ven Marl Member, Stonebarrow, Charmouth comprising medium and dark grey claystones and shales. Person standing on Limestone with Brachiopods (Bed 87) at base and Stellare Nodules (Bed 88f) at head level. C. The Belemnite Stone (Bed 121) and silty grey mudstones of the Green Ammonite Beds at Seatown, UK showing faint cyclicity.

Figure 3. CL photomicrographs (A, B) of non-luminescent rostrum (*Passaloteuthis*) with luminescent apical line area (sample B26); (C) luminescent apical line area of *Passaloteuthis* rostrum (Sample BE11); (D) non-luminescent rostrum (*Passaloteuthis*) with luminescent sparry calcite margin (Sample BE0995). (E) non-luminescent rostrum (*Hastites*) within luminescent margin and within luminescent crinoidal skeletal material (Sample BC28C) (F) non-luminescent rostrum (*Nannobelus*) within luminescent sediment (Sample BVM10).

Figure 4. Cross plot of $\delta^{18}O$ and $\delta^{13}C$ data from the belemnite specimens (*Nannobelus*, *Hastites* (including *Pseudohastites turris)*, *Bairstowius* and *Passaloteuthis* (including *Pseudopassaloteuthis ridgensis*).

Figure 5. Oxygen isotopes (and 8–point running mean), carbon isotopes (and 8–point running mean), Mg/Ca ratios (and 5–point running mean) and TOC, through the studied interval. Grey shaded areas represent the 95% confidence interval. Biostratigraphy after Cope et al. [1980], Hesselbo and Jenkyns [1995] and Page [1992] and bed numbers after Lang and Spath [1926] and Lang et al. [1928]. Constraints placed on the negative excursions are marked with minimum duration [from cyclostratigraphic timescale of Weedon and Jenkyns, 1999]. TOC data from Weedon and Jenkyns [1999]and Jenkyns and Weedon [2013]. Brevis = Brevispina; Mass = Masseanum; Vald = Valdani; Lurid = Luridum; Macul = Maculatum Subzone.

Figure 6. Chemostratigraphic correlation of the Dorset succession with data from the Cleveland Basin, [Korte and Hesselbo, 2011]; the Madonna della Corona section [Woodfine et al., 2008]; the Viote section [Franceschi et al., 2014; the Basque–Cantabrian Basin[Rosales et al., 2006] and San Pedro de Moel [Duarte et al., 2014] and Peniche [Oliveira et al., 2006]. The prominent positive carbon isotope event seen within the Ibex Zone is highlighted.

Figure 1. Figure

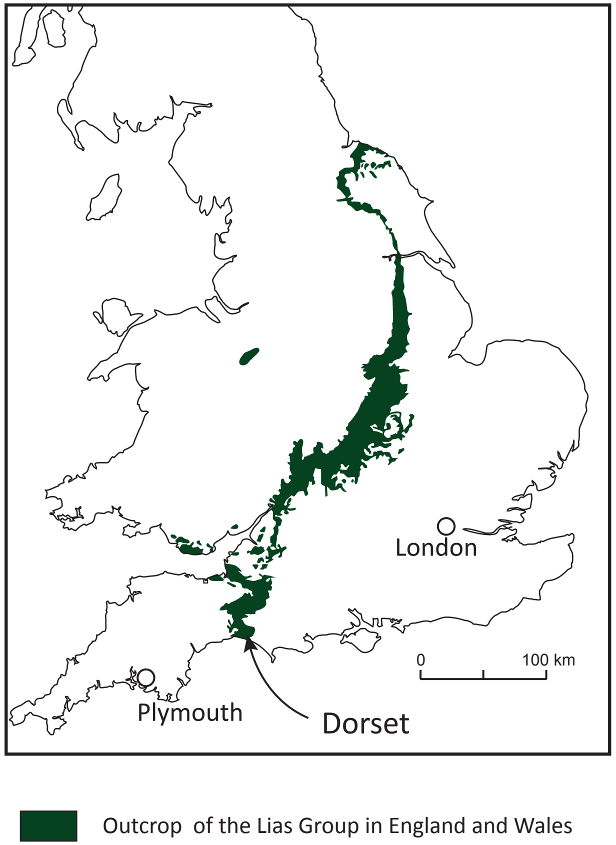
London
Plymouth
Dorset
0
100 km
Outcrop of the Lias Group in England and Wales

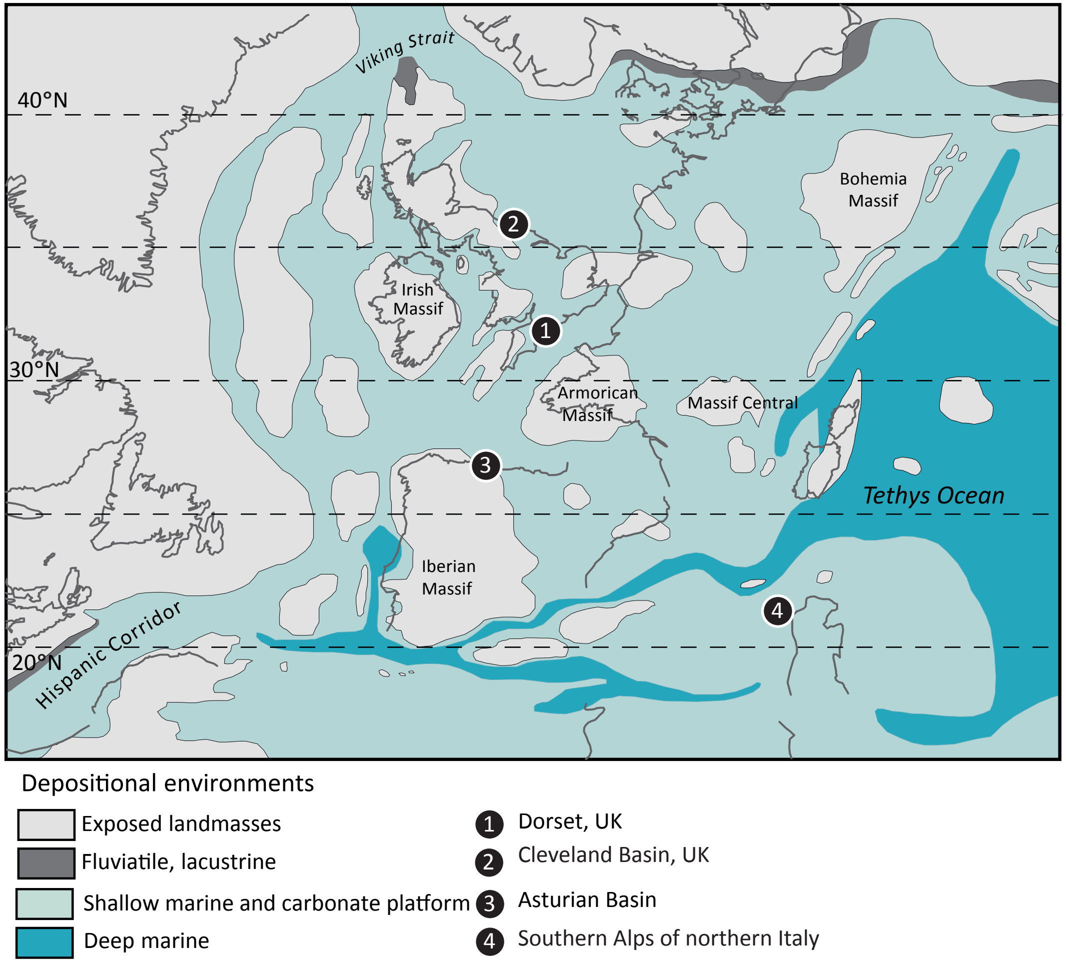
Viking Strait
40°N
30°N
20°N
Bohemia Massif
Irish Massif
Armorican Massif
Massif Central
Iberian Massif
Tethys Ocean
Hispanic Corridor
Depositional environments
Exposed landmasses
Fluviatile, lacustrine
Shallow marine and carbonate platform
Deep marine
1 Dorset, UK
2 Cleveland Basin, UK
3 Asturian Basin
4 Southern Alps of northern Italy

Figure 2. Figure

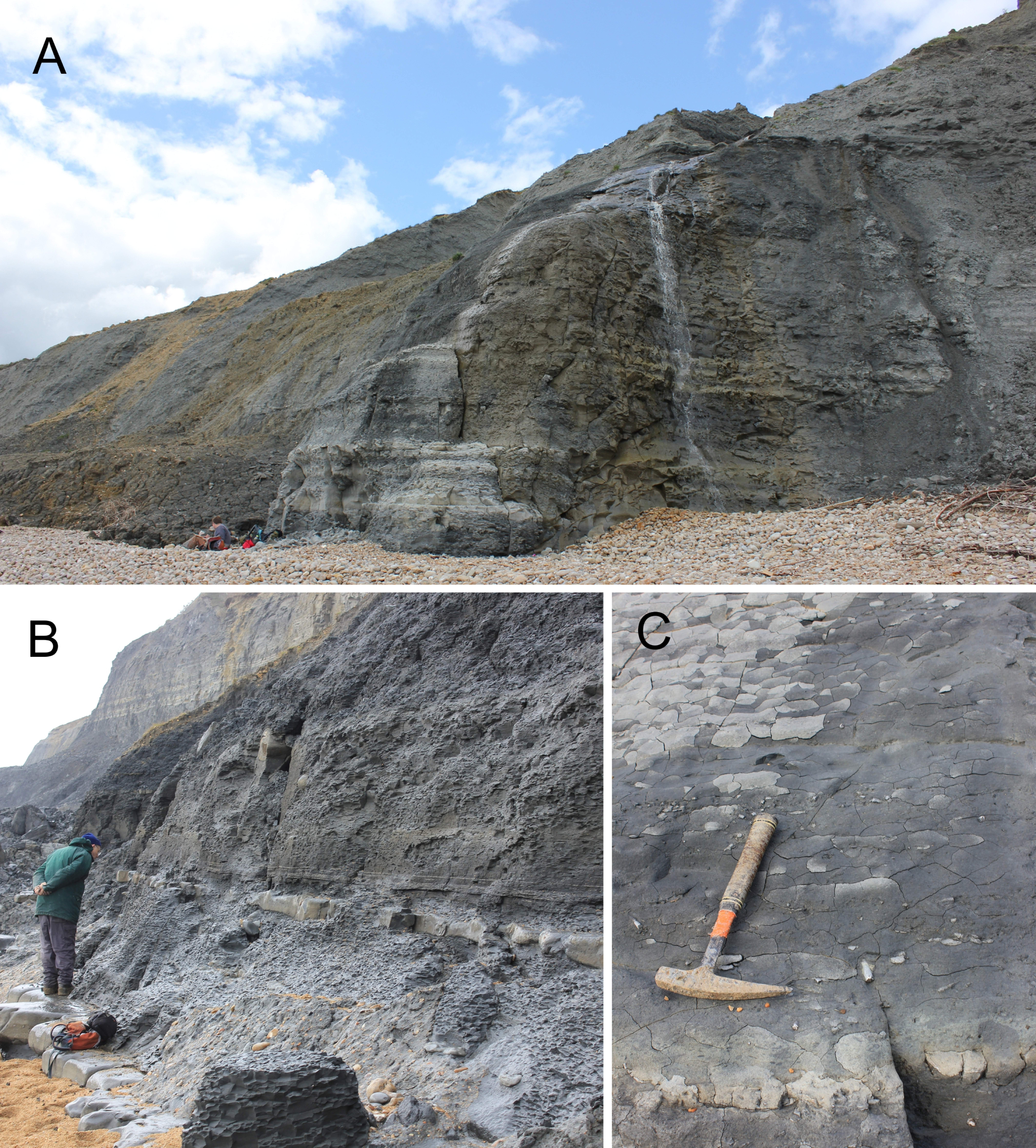
A
B
C

Figure 3. Figure

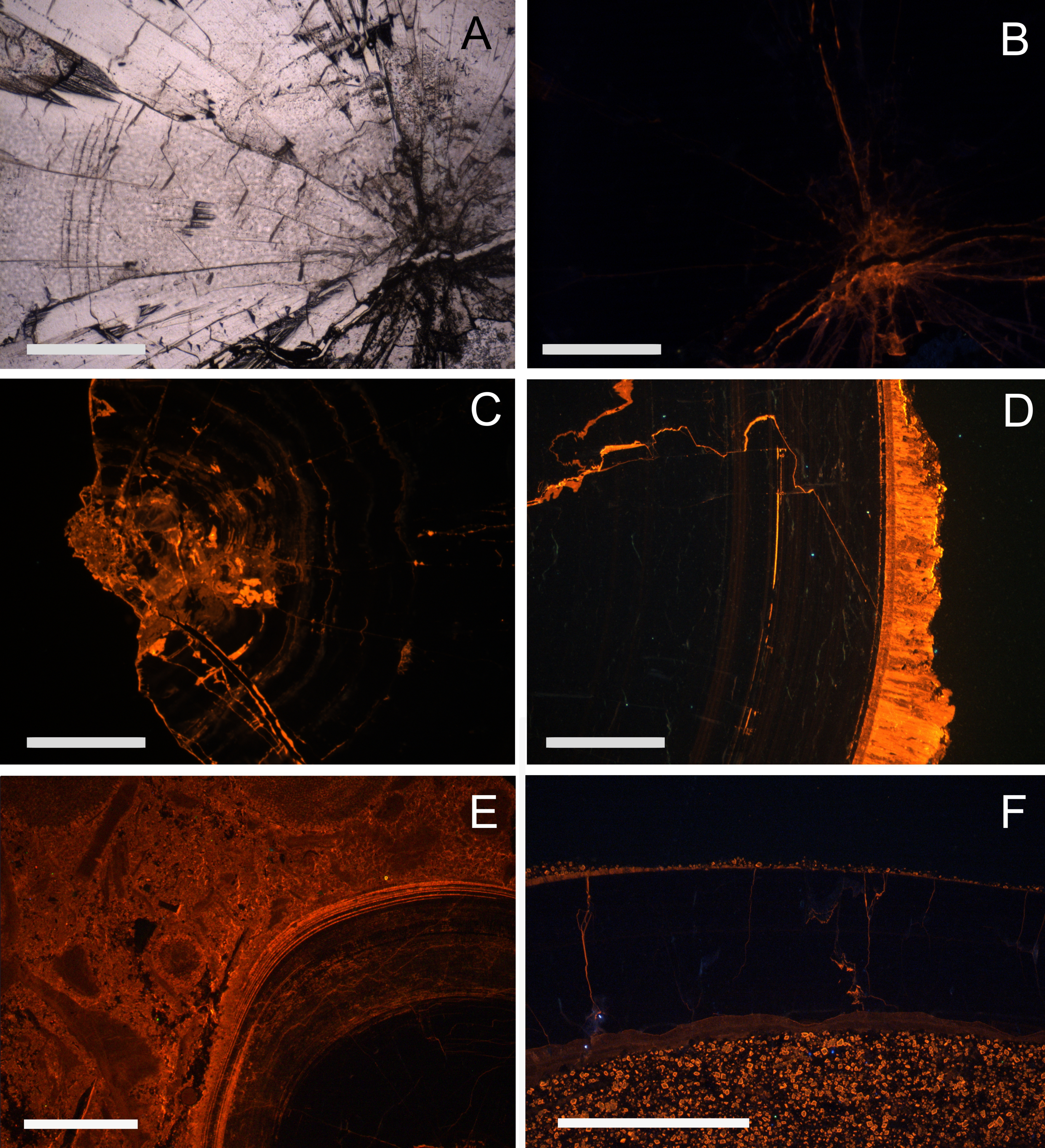
A
B
C
D
E
F

Figure 4. Figure

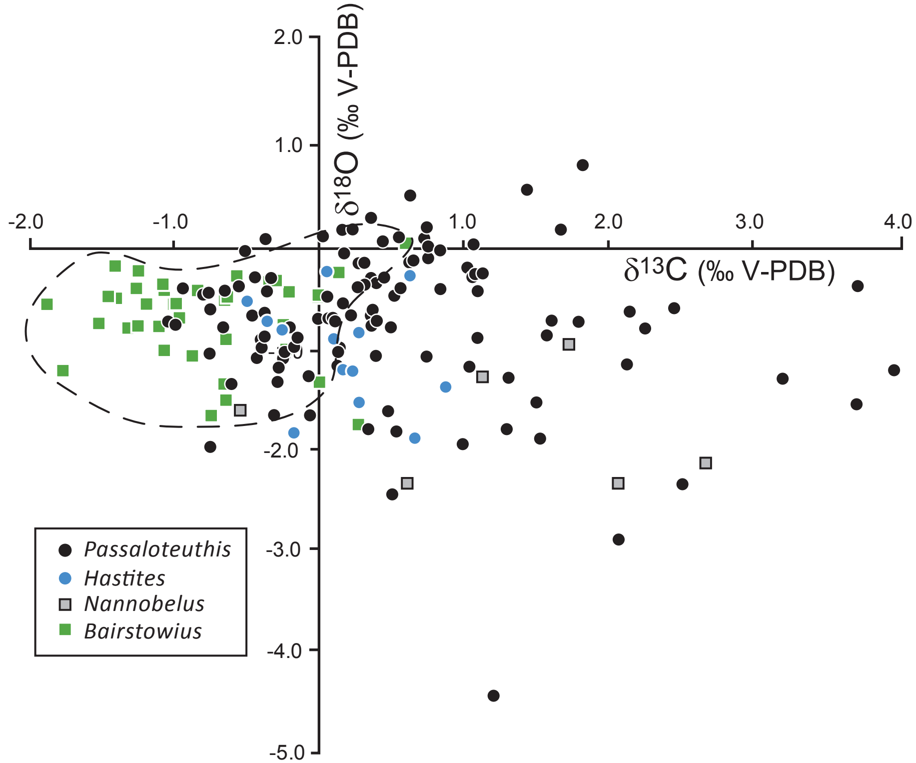

δ18O (‰ V-PDB)
δ13C (‰ V-PDB)
2.0
1.0
-2.0
-3.0
-4.0
-5.0
-2.0
-1.0
1.0
2.0
3.0
4.0
Passaloteuthis
Hastites
Nannobelus
Bairstowius

Figure 5.

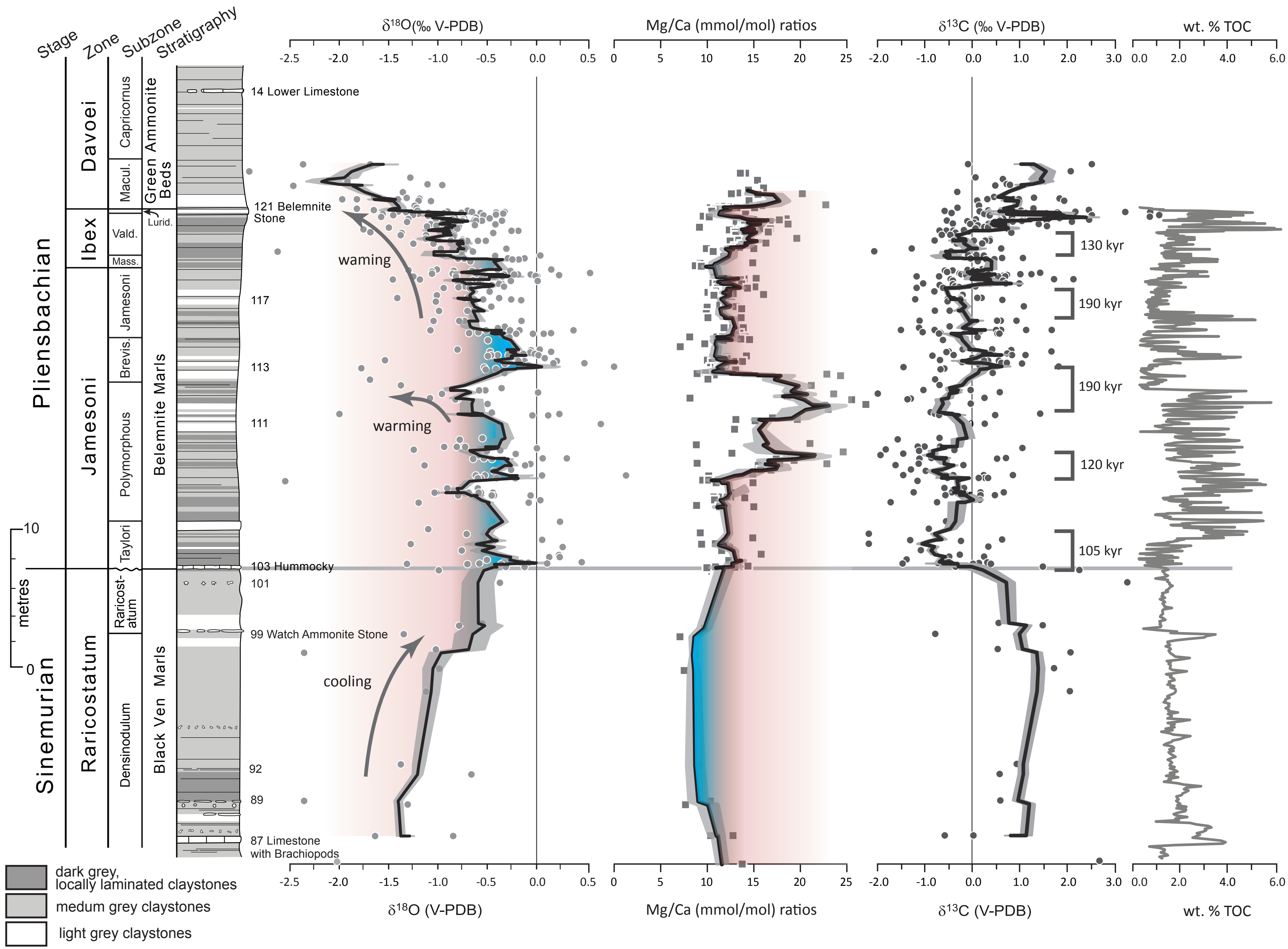

Stage
Zone
Subzone
Stratigraphy
Pliensbachian
Sinemurian
Davoei
Ibex
Jamesoni
Raricostatum
Capricornus
Macul.
Vald.
Mass.
Jamesoni
Brevis.
Polymorphous
Taylori
Raricost-atum
Densinodulum
Green Ammonite Beds
Lurid.
Belemnite Marls
Black Ven Marls
14 Lower Limestone
121 Belemnite Stone
117
113
111
103 Hummocky
101
99 Watch Ammonite Stone
92
89
87 Limestone with Brachiopods
10
metres
0
δ18O(‰ V-PDB)
Mg/Ca (mmol/mol) ratios
δ13C (‰ V-PDB)
wt. % TOC
-2.5 -2.0 -1.5 -1.0 -0.5 0.0 0.5
0 5 10 15 20 25
-2.0 -1.0 0.0 1.0 2.0 3.0
0.0 2.0 4.0 6.0
waming
warming
cooling
130 kyr
190 kyr
190 kyr
120 kyr
105 kyr
δ18O (V-PDB)
Mg/Ca (mmol/mol) ratios
δ13C (V-PDB)
wt. % TOC
dark grey, locally laminated claystones
medum grey claystones
light grey claystones

Figure 6.

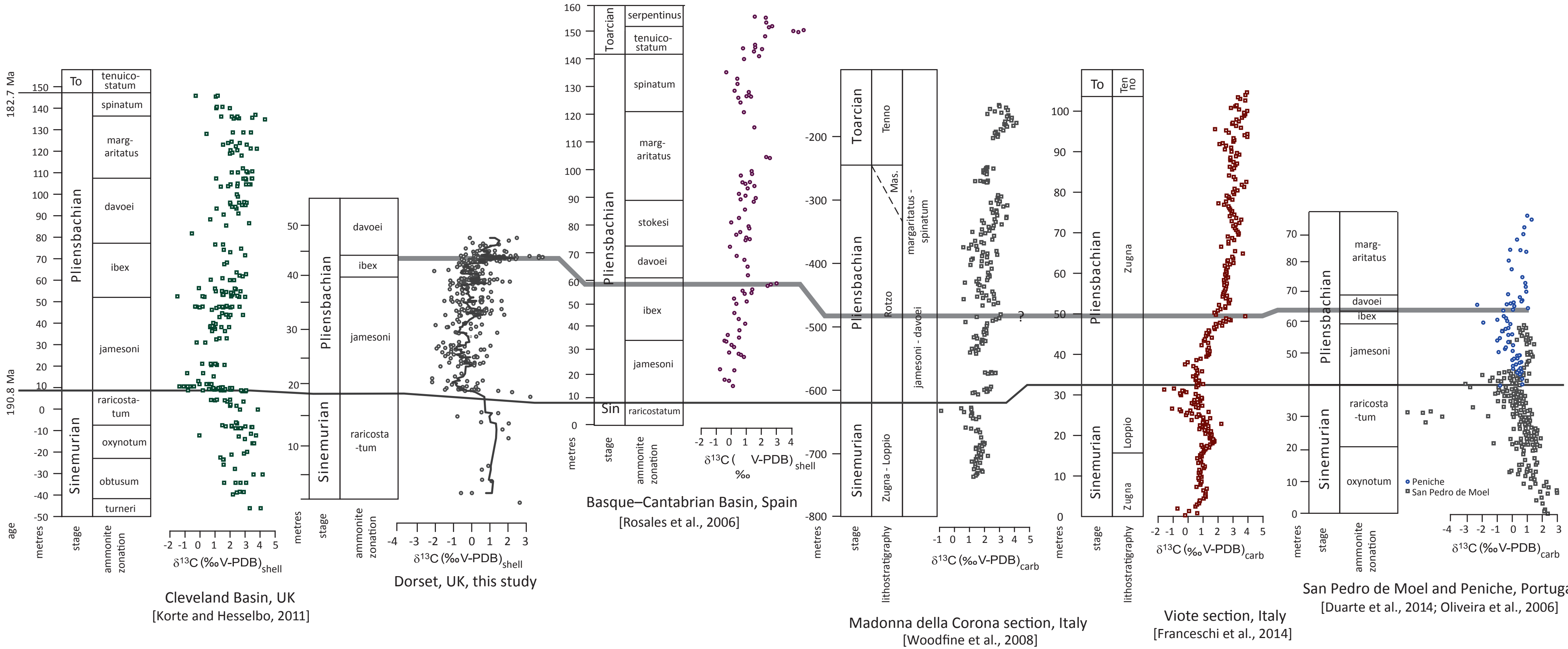

Cleveland Basin, UK
[Korte and Hesselbo, 2011]
Dorset, UK, this study
Basque–Cantabrian Basin, Spain
[Rosales et al., 2006]
Madonna della Corona section, Italy
[Woodfine et al., 2008]
Viote section, Italy
[Franceschi et al., 2014]
San Pedro de Moel and Peniche, Portugal
[Duarte et al., 2014; Oliveira et al., 2006]
182.7 Ma
190.8 Ma
age
metres
stage
ammonite zonation
lithostratigraphy
Toarcian
Pliensbachian
Sinemurian
To
Sin
tenuicostatum
serpentinus
spinatum
margaritatus
stokesi
davoei
ibex
jamesoni
raricostatum
oxynotum
obtusum
turneri
Tenno
Mas.
Rotzo
Zugna - Loppio
Zugna
Loppio
margaritatus - spinatum
jamesoni - davoei
Peniche
San Pedro de Moel
δ13C (‰V-PDB)shell
δ13C (‰V-PDB)carb